INORGANIC CHEMISTRY FRONTIERS

RESEARCH ARTICLE

View Article Online
View Journal | View Issue

Cite this: *Inorg. Chem. Front.*, 2025, **12**, 7421

The complexation and solvent extraction properties of a phenanthroline diamide extractant for trivalent actinide and lanthanide ions†

Emma M. Archer, [a] Felipe A. Pereiro, [a,b] Jocelyn M. Riley,[a] Jacob P. Brannon, [a] Elizabeth B. Flynn,[a] J. Connor Gilhula, [b] Brittany L. Huffman, [b] Jessica A. Jackson, [a] Julia G. Knapp, [b] Brian N. Long, [b] Harris E. Mason, [b] Monica S. Mullis, [b] Stosh A. Kozimor, *[b] Jenifer C. Shafer *[a] and Shane S. Galley *[a]

The study of trivalent actinide (An(III)) interactions with nitrogen and oxygen donor (N,O-donor) extractants is highly relevant to efforts aimed at closing the nuclear fuel cycle. Despite their importance, extraction of transplutonium actinides remains underexplored. A popular N,O-donor extractant, phenanthroline diamide (DAPhen), has incurred interest for f-element separations due to numerous positive qualities such as molar acid stability, a pre-organized binding mode, and tunable amide functionalities. Solvent extraction experiments of TEtDAPhen in nitrobenzene demonstrated selectivity for multiple An(III) (An = Am, Cm, Bk, Cf) metals over Eu(III). Surprisingly, extraction efficiency did not follow periodic trends. Extraction was most effective for Am(III), followed by Cf(III) ≈ Bk(III), and lowest for Cm(III). To provide additional insight into the extraction process, coordination chemistry studies were conducted between Am(III) and numerous Ln(III) cations (Pr(III), Nd(III), Tb(III), Lu(III)) with TEtDAPhen. Lanthanide speciation and stability constants were measured using UV-Visible spectroscopy which showed increasing stability constants from Nd(III)–Gd(III) with consistent one-to-one metal-to-ligand stoichiometry. Single crystal X-ray crystallography studies of M(TEtDAPhen)$(NO_3)_3$ complexes confirmed these findings. Collectively, these results highlight the potential of DAPhen-based extractants for selective An(III) separations and contribute to a deeper understanding of f-element coordination behavior.

Received 2nd May 2025,
Accepted 2nd July 2025

DOI: 10.1039/d5qi01056j

rsc.li/frontiers-inorganic

Introduction

Nuclear energy has been gaining momentum as an alternative energy source due to lower CO_2 emissions than fossil fuel combustion technologies.[1] However, numerous challenges exist that prevent widespread implementation of this technology. One challenge is related to the fate of used nuclear fuel (UNF). Consider that UNF is rich in energy content. It retains 95% of the energy value after being removed from a commercial reactor. The challenge lies in recovering the fissionable radionuclides from other waste in the fuel *via* a chemical recycling process.[2] For radionuclides such as uranium and plutonium, this recovery process is established.[3] For the minor actinides (Am(III) and Cm (III)), recovery efforts are often ineffective because purification from lanthanide fission product contaminants is challenging.[4,5] Identifying methods that cleanly separate An(III) from Ln(III) would drastically reduce the radiological and thermal hazards of nuclear power waste and enable additional and substantial energy content to be further extracted from the used fuel.[6,7]

The separation of An(III) from Ln(III) is quite difficult because these elements have similar chemical properties.[6,8–10] There have been many advances in this area over the years using mixed N,O-donor extractants that exploit covalent bonding inter-

[a]*Department of Chemistry, Colorado School of Mines, Golden, Colorado 80401, USA. E-mail: jshafer@mines.edu, sgalley@mines.edu*
[b]*Los Alamos National Laboratory, Los Alamos, New Mexico 87545, USA. E-mail: stosh@lanl.gov*

†Electronic supplementary information (ESI) available. CCDC 2385181–2385185. For ESI and crystallographic data in CIF or other electronic format see DOI: https://doi.org/10.1039/d5qi01056j

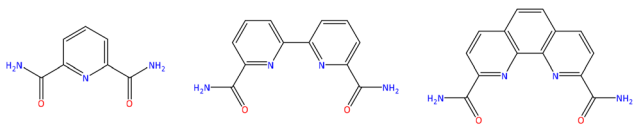

Fig. 1 Structures of amide functionalized pyridine (left), bipyridine (middle), phenanthroline (right).

actions with An(III) to achieve separation.[5,11,12] Recent studies have demonstrated that N-donor ligands, (*e.g.* amide functionalized pyridine- and bipyridine-based extractants, shown in Fig. 1) and mixed N,O-donor ligands have extraction selectivity for An(III) over Ln(III).[4,13–17] Frequently, the nitrogen interaction with the metal center is thought to induce selectivity for An(III) over Ln(III) explained by the hard soft acid base theory.[13,18] Another potentially attractive attribute is associated with the rigidity of the N-heterocyclic backbone. This structural feature may predispose these extractants for metal binding, improving both kinetics and complex stability.[19,20]

One particularly interesting sub-class of N,O-donor extractants is the phenanthroline diamide (DAPhen) compounds (Fig. 1). These extractants preferentially bind 5*f* An(III) ions over 4*f* Ln(III) ions and are capable of separating actinides from lanthanides *via* solvent extraction.[21,22] Many studies have shown high separation factors for removing Am(III) from Eu(III) and few have shown the separation of Am(III) from Cm(III).[23–25] These results suggest that equally impressive separation factors could be exhibited by later transplutonium elements, like Bk(III)and Cf(III).

In the present work, *N*,*N*,*N*′,*N*′-tetraethyl-1,10-phenanthroline-2,9-diamide (TEtDAPhen) was synthesized and solvent extraction with Am(III), Cm(III), Bk(III), Cf(III), and Eu(III) was explored in nitrobenzene. These data showed TEtDAPhen was effective at extracting An(III); however, the extent of the An(III) extraction was not periodic. Instead, extraction was the highest for Am(III), followed by Cf(III) and Bk(III), and the lowest for Cm (III). The extraction of Eu(III) was explored for comparison and was extracted to a much lower extent compared to the An(III). In addition, complexation of Am(III) and Ln(III) cations (Pr(III), Nd(III), Tb(III), Lu(III)) with TEtDAPhen was explored through X-ray crystallography and Ln(III) speciation and stability constants with Nd(III), Eu(III), and Gd(III) were measured. A consistent one-to-one metal-to-ligand stoichiometry was observed in the solution and solid-state studies. Collectively, these data suggest DAPhen-based extractants are exceptionally suited for separating An(III) from Ln(III) *via* solvent extraction. The data is presented within the context of other relevant phenanthroline studies recently published in literature.[26–29]

Results and discussion

Solvent extraction

Liquid–liquid solvent extraction experiments are achieved by utilizing an aqueous immiscible organic phase containing an extractant that can selectively bind to metals in the acidic aqueous phase. This is best achieved by the extractant binding in the inner coordination sphere to extract the metal into the organic phase.[30] By measuring the partitioning of a metal from the aqueous phase to the organic phase, liquid–liquid solvent extraction represents metal–ligand coordination.[31]

The solvent extraction capabilities of TEtDAPhen were evaluated with Am(III), Cm(III), Bk(III), Cf(III), and Eu(III) in nitrobenzene. This solvent provided ample solubility for the TEtDAPhen extractant and allowed comparison with other extractants evaluated in the literature, like F-3 (3-nitrobenzotrifluoride) while providing cost effectiveness and solubility similarities.[32,33] Equilibrium was reached by a contact time of 60 minutes on a shaker table which is a mechanical device that shakes vials for thorough mixing of the aqueous and organic phases. This procedure was followed to achieve consistency between this work and published work. To measure metal partitioning from the aqueous to the organic phase, the distribution ratio (*D*) was measured, as defined in eqn (1). To determine the concentration of acid that results in a *D* value that generates the lowest error, acid dependency experiments were performed. These were done by measuring the metal distribution at varying acid concentrations while maintaining one ligand concentration. It was found that the highest distribution values were obtained at an aqueous phase concentration of 3 M HNO_3 (shown in Fig. S2 and S3†).

$$D = \frac{[M]_{org}}{[M]_{aq}} \quad (1)$$

As shown in Fig. 2, Am(III) had the highest distribution values, followed by Cf(III), Bk(III), Cm(III), and then Eu(III). These results indicate higher selectivity for Am(III) and are consistent with literature results for DAPhen extractants.[34,35] The slope values of the logarithmic plot in Fig. 2 are 1.14 ± 0.04 for Eu(III), 1.12 ± 0.02 for Am(III), 1.29 ± 0.09 for Cm(III), 1.10 ± 0.01 for Bk(III), and 1.09 ± 0.02 for Cf(III) indicating that the ligand-to-metal stoichiometry of the extracted species was primarily one-to-one in nitrobenzene. The Cm(III) slope of 1.29 ± 0.09 indicates a possibility of the presence of a one-to-two extracted species while the one-to-one is the dominant species. Based on the solid-state structures (*vide infra*), we assume no bound waters to the extracted species. The slope values or solvation numbers for TEtDAPhen with Eu(III), Am(III), Cm(III), Bk(III), and Cf(III) are similar to the butyl alkylated TBuDAPhen extractant studied (in F-3) by Alyapyshev *et al.* who reported slopes of 1.1 and 1.2 for Eu(III) and Am(III), respectively.[35] The solution phase speciation from TEtDAPhen was also different than the

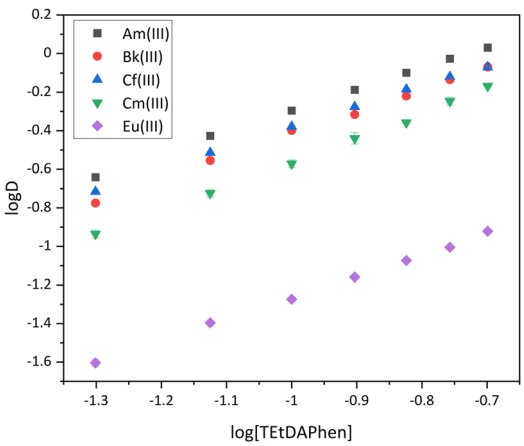

Fig. 2 Ligand concentration dependency of TEtDAPhen with Am(III), Cm(III), Bk(III), Cf(III), and Eu(III).

dodecyl alkylated TDoDecDAPhen extractant studied by Tsutsui *et al.* Those researchers determined solvation numbers for the TDoDecDAPhen extraction of Eu(III), Am(III), and Cm(III) to be 1.2, 1.4, and 1.5 in nitrobenzene, respectively.[32] These data suggested that the TDoDecDAPhen extracted species had a mixed stoichiometry of one-to-one and one-to-two, which is distinct from TEtDAPhen.

The separation factors (SF) of TEtDAPhen in nitrobenzene were consistent over the concentration range of TEtDAPhen. For Am(III) over Eu(III), $SF_{Am/Eu}$ did not change substantially as the TEtDAPhen concentration was varied. They ranged from 9.5 to 8.9 with an average of 9.3 with a standard deviation of 0.3 (at 1σ; Fig. 3 and Table 1). Similar TEtDAPhen concentration independence was observed for Cm(III), with $SF_{Cm/Eu}$ that ranged from 5.7 to 4.7 and averaged to 5.2 ± 0.3. Comparing these data with other phenanthroline based extractants demonstrated that TEtDAPhen was reasonably effective at removing Am(III) and Cm(III) from Eu(III). For instance, the $SF_{Am/Eu}$ for TEtDAPhen in nitrobenzene is higher than TBuDAPhen in F-3 (8.9) whereas the $SF_{Am/Cm}$ is higher for TBuDAPhen in F-3 (2.6).[35,36] In contrast, longer alkylated DAPhen extractants like the decylated TDecDAPhen and the dodecylated TDoDecDAPhen reported higher $SF_{Am/Eu}$ under a variety of experimental conditions: low acid concentration and high ionic strength as well as high acid concentration and high ionic strength. The TDoDecDAPhen (nitrobenzene) in a molar concentration acid system performed similarly to TEtDAPhen with a $SF_{Am/Eu}$ of 8.7, whereas TDecDAPhen (*n*-dodecane–*n*-octanol (5 : 1)) in a low acid and high ionic strength system exceeded TEtDAPhen with a $SF_{Am/Eu}$ of 51.[32,37] For separation applications, these data suggest DAPhen extractants with long alkyl chains have higher selectivity for Am(III) over Eu(III). Some of these differences likely arise from improved solubility of the longer alkylated DAPhen extractants in organic diluents. Further investigation of this phenomenon is required for the other An(III) ions.

The ability of TEtDAPhen to separate adjacent actinides, Am(III) and Cm(III), was also investigated (Fig. 3). The solvent extraction data in nitrobenzene showed $SF_{Am/Cm}$ ranged from 2.0 to 1.6 over the tested TEtDAPhen concentration range with an average of 1.8 ± 0.1. These SF values are comparable with other extractants that have been tested for this difficult minor actinide separation. Of the DAPhen class of ligand, Et(pHexPh)ClPhen has the highest Am(III) over Cm(III) SF value in the literature of 6.5 at 0.5 M HNO_3.[36] The asymmetric alkyl and aryl substituted DAPhen extractants have shown higher SFs compared to the alkylated DAPhens.

This study was extended to Bk(III) and Cf(III) to investigate the heavier actinide interactions with TEtDAPhen. It was observed that the selectivity of TEtDAPhen for Bk(III) and Cf(III) was close to that of Am(III) where the extraction of Bk(III) and Cf(III) was nearly identical. Over the tested TEtDAPhen concentration range, the $SF_{Bk/Eu}$ ranged from 7.4 to 6.8 with an average of 7.1 ± 0.2 while the $SF_{Cf/Eu}$ ranged from 7.9 to 7.1 with an average of 7.6 ± 0.2 (Table 1). These SFs further show selectivity of TEtDAPhen for the An(III) over the Ln(III).

The lack of periodicity in the extraction behavior of the An(III) has implications for interesting electronic differences between the An(III) from Am(III)–Cf(III) which require further study.

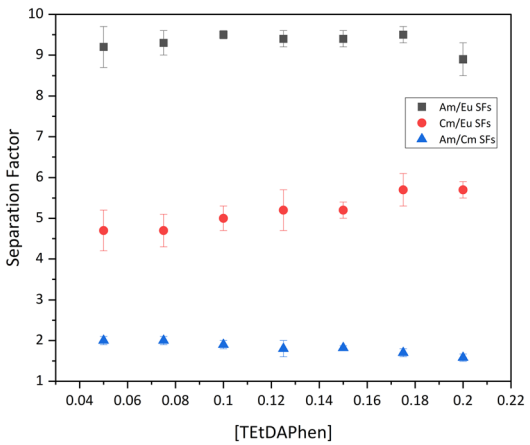

Fig. 3 Separation factors of Am(III), Eu(III), and Cm(III) using TEtDAPhen ([TEtDAPhen] = 0.05 M–0.2 M).

Table 1 Calculated separation factors with the standard deviation reported as the uncertainty

Separation	Separation factor value
$SF_{Am/Eu}$	9.3 ± 0.3
$SF_{Cm/Eu}$	5.2 ± 0.3
$SF_{Bk/Eu}$	7.1 ± 0.2
$SF_{Cf/Eu}$	7.6 ± 0.2
$SF_{Am/Cm}$	1.8 ± 0.1

UV-Visible spectrophotometric titration

To test the effect of metal ion charge density on the complexation chemistry of TEtDAPhen, the reactions between TEtDAPhen and a series of Ln(III) cations were investigated. This was achieved by conducting spectrophotometric titrations of Ln(III) with TEtDAPhen. Because the Ln(III) ionic radius methodically decreases across the series, the Ln(III) cations charge density systematically increases from Nd(III) to Eu(III) to Gd(III), enabling us to probe the impact of charge density on stability of complexation with TEtDAPhen.[35,36] The UV-Vis spectra obtained from solutions that contained TEtDAPhen and Nd(III), Eu(III), and Gd(III) were similar and dominated by strong transitions of TEtDAPhen observed between 240–380 nm.

Similar observations have been made and documented in the literature for other DAPhen extractants.[29,34,38,39] As a metal containing solution was titrated into the ligand solution, complexation was observed in the resulting spectra, shown in Fig. 4. The complexation was evident from the decrease in intensity of the main TEtDAPhen peak at 273 nm accompanied by an increase in intensity of peaks near 253 nm and 295 nm.

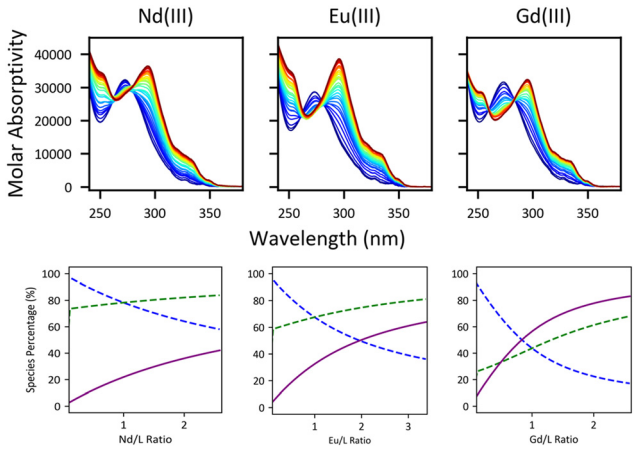

Fig. 4 (Top) Spectrophotometric titrations of TEtDAPhen with Nd$(NO_3)_3$ (left), Eu$(NO_3)_3$ (middle), and Gd$(NO_3)_3$ (right) in methanol. $[TEtDAPhen]_i$ = 0.02 mM, $[Nd(NO_3)_3]_i$, $[Eu(NO_3)_3]_i$, and $[Gd(NO_3)_3]_i$ = 0.45 mM. V_i = 1 mL of TEtDAPhen with 5 μL additions of Nd$(NO_3)_3$, Eu$(NO_3)_3$, and Gd$(NO_3)_3$, respectively. (Bottom) Speciation diagram of the formation of the M(TEtDAPhen)$(NO_3)_3$ complexes with free metal (green dash), free ligand (blue dash), and complex (purple) plotted.

Two isosbestic points were also observed near 260 nm and 282 nm, indicating two absorbing species verified by factor analysis (free ligand and one complex). The titration data were fit using a spectrophotometric fitting program, HypSpec2014, and the stability constants ($\log\beta$) for a one-to-one Ln(III) : TEtDAPhen complex obtained (Table 2).[40,41]

These stability constants, which inform on the binding affinity of TEtDAPhen for different metal ions, were positively correlated with charge density of the Ln(III) cation. The Gd(III) cation, the highest charge density of the cations that were investigated, showcased the highest stability constant (5.19 ± 0.01). In contrast, the larger and less charge dense Eu(III) cation had a lower stability constant (4.57 ± 0.02). The lowest stability constant was observed for the largest and least charge dense Nd(III) cation (4.27 ± 0.01).

Comparing these TEtDAPhen stability constants with other DAPhen extractants revealed similar stability constants to 4,7-dichloro-F_3MePyr-DAPhen and F_3MePyr-DAPhen but different stability constants compared to TMDAPhen. For example, the tetramethylated DAPhen ligand, TMDAPhen, reported in literature in MeOH/10% (v) H_2O showed an opposite trend where the Nd(III) $\log\beta$ values were higher than the Eu(III) values; however, the stability constants for the one-to-one $\log\beta$ values were within error of each other. The one-to-one $\log\beta$ value for Eu(III) with TEtDAPhen (4.57) indicated that a weaker complex formed than the one-to-one complex of TMDAPhen (5.82).[42] The trend of increasing stability constants across the Ln series has been observed for the aryl substituted 4,7-dichloro-F_3MePyr-DAPhen and F_3MePyr-DAPhen, indicating this is a trend for the DAPhen extractants as a result of the increasing charge density of the later Ln(III) and the investigation of these systems in a monophasic system.[43]

Complexes with one-to-one stoichiometry fit well in HypSpec2014 and factor analysis revealed only two absorbing species for the TEtDAPhen system – the free ligand and the one-to-one metal-to-ligand complex. The increase in one-to-one stability constants from Nd(III) to Gd(III) indicates that the stability of the complex may depend on the metal ion size in addition to the steric constraints that the ethyl chains on the amide arms contribute.

Table 2 Measured stability constants in methanol with TEtDAPhen reported at the 95% confidence level

Reaction	$\log\beta$
TEtDAPhen + Nd^{3+} ⇋ Nd(TEtDAPhen)$^{3+}$	4.27 ± 0.01
TEtDAPhen + Eu^{3+} ⇋ Eu(TEtDAPhen)$^{3+}$	4.57 ± 0.02
TEtDAPhen + Gd^{3+} ⇋ Gd(TEtDAPhen)$^{3+}$	5.19 ± 0.01

X-ray crystallography

A crystallographic study of the TEtDAPhen extractant was explored to validate the An(III)-to-TEtDAPhen and Ln(III)-to-TEtDAPhen stoichiometries determined above by slope analysis from the solvent extraction data and by UV-Vis spectrophotometric titration. Toward this end, Am(III) and Ln(III) (Ln = Pr, Nd, Tb, Lu) nitrates representative of the Ln(III) series were dissolved in acetonitrile and mixed with one equivalent of TEtDAPhen, also in acetonitrile (Scheme 1). Vapor diffusion with diethyl ether overnight resulted in the formation of suitable crystals for X-ray diffraction. Obtaining a structure with Am(III) was of particular interest, due to the selectivity shown by TEtDAPhen. This examination allows for direct structural characterization with the Ln(III) and can set precedence for further studies with the An(III).

These data showed that one-to-one M(III)-to-TEtDAPhen complexes formed. Additional experiments were carried out with Ln(III) cations to probe the formation of one-to-two complexes. Adding more equivalents of TEtDAPhen provided no evidence for formation of one-to-two adducts.

Analysis of X-ray diffraction studies revealed a 10-coordinate bicapped square antiprism geometry about the Am(III), Pr(III), Nd(III), and Tb(III) metal centers (crystallographic Tables S1–S3 and S5†). The first coordination sphere is defined by tetradentate coordination of the TEtDAPhen ligand and three coordinating nitrates binding in a bidentate fashion. The coordination of these structures is consistent with other DAPhen ligand systems where crystals are grown with metal nitrates.[38,44]

The molecular structure M(TEtDAPhen)$(NO_3)_3$ [M = Am(III), Pr(III), Nd(III), Tb(III)] is shown in Fig. 5. The M–O_L (O_L refers to

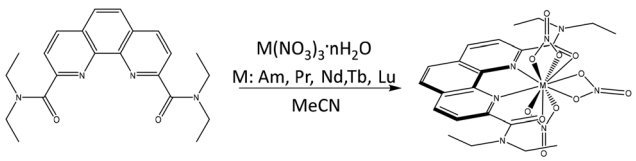

Scheme 1 Synthetic schematic of formation of M(TEtDAPhen)$(NO_3)_3$.

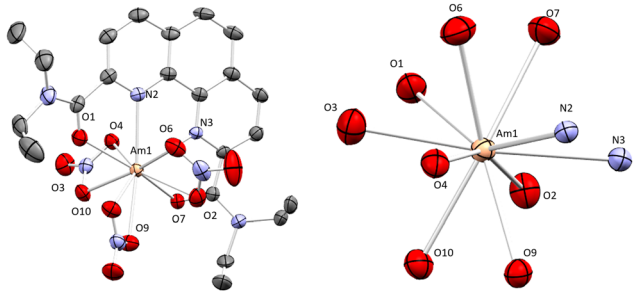

Fig. 5 The structure of Am(TEtDAPhen)$(NO_3)_3$ shown as 30% probability ellipsoids. Hydrogens were omitted for clarity (left). The 10-coordinate metal center shows the coordination of oxygen and nitrogen (right).

the O atoms of the TEtDAPhen ligand) bond lengths are 2.466(4) and 2.424(4) Å for Am(III), 2.477(2) and 2.463(3) Å for Pr(III), 2.4745(10) and 2.4119(11) Å for Nd(III), and 2.3617(11) and 2.4210(11) Å for Tb(III). In the Am(III), Nd(III), and Tb(III) structures, asymmetry in the M–O_L bond exists where one oxygen bond is shorter than the other. This is not observed in the Pr(III) structure to the same extent. The similarity of structures between Am(III) and Nd(III) is expected owing to their similar ionic radii. Asymmetry of the M–N bond lengths is also observed in this system, except for the Pr(III) structure. The M–N bond lengths are 2.594(5) and 2.655(5) Å for Am(III), 2.650(3) and 2.652(3) Å for Pr(III), 2.6126(12) and 2.6738(11) Å for Nd(III), and 2.5484(12) and 2.6088(12) Å for Tb(III). The same asymmetry is observed with the M–N distances in the Am(III), Nd(III), and Tb(III) structures compared to the M–O_L distances.

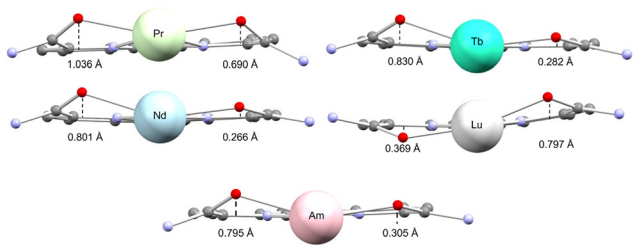

Fig. 6 Distance of M–O_L bonds from the plane of the phenanthroline backbone.

In comparison to the previously reported M(TBuDAPhen) system, the M–O_L and M–N distances are comparable and within error of the bond distances observed for the M(TEtDAPhen) system [M = Pr(III), Nd(III), Tb(III)].[44]

Looking further, the asymmetric bonding of the Am(III), Nd(III), and Tb(III) structures in comparison to the Pr(III) structure was apparent within the M–O_L bonds. In the case of the Pr(TEtDAPhen)$(NO_3)_3$ complex, the M–O_L bonds are bent out of the plane of the phenanthroline moiety at distances of 1.036 Å and 0.690 Å shown in Fig. 6. This distortion leads to nearly symmetrical bonding within the Pr(III) system. In contrast, the distances of the Am–O_L bonds from the phenanthroline planes are 0.795 Å and 0.305 Å matching closely to the distortion of the Nd–O_L bonds from the phenanthroline plane with distances of 0.801 Å and 0.266 Å. As a result of this distortion in bonding, asymmetrical bond lengths arise in the structures of Am(III), Nd(III), and Tb(III) which are attributable to the effects of cation size. This is not unusual for the DAPhen family of ligands as this distortion has been previously reported.[44] For the TBuDAPhen system, both oxygen atoms remain out of plane until Ho(III) and are closer to the plane at Er(III).[44] In this work, the distortion break is observed earlier in the series at Nd(III). This distortion may result from steric hinderance of the less-flexible ethyl chains on the amide arms in comparison to the TBuDAPhen system in conjunction with size of the metal ion. These differences lead to different geometries of the metal centers in the molecular Ln(III) complexes.

The crystallographic data for Am(III), Pr(III), Nd(III), and Tb(III) reveal three, bidentate nitrate anions coordinating to the metal center (see Fig. 5). The bond lengths of Pr–$O_{(NO_3)}$ range from 2.527(3)–2.568(11), those of Nd–$O_{(NO_3)}$ range from 2.5186(10)–2.5866(11), those of Am–$O_{(NO_3)}$ range from 2.521(4)–2.584(5), and those of Tb–$O_{(NO_3)}$ range from 2.4439(10)–2.5341(12) Å (see Table 3). The M–$O_{(NO_3)}$ bond lengths decrease as lanthanide cation size decreases. The tris-nitrato complex's bond lengths are comparable to the reported structures containing three nitrates.[45] In the case of Tb(III), the bond distance of the N–O bond in the equatorial plane is longer than anticipated, showing a possible change in coordination later in the Ln(III) series after Tb(III).

The Lu(III) crystallographic data reveals a nine-coordinate geometry where two nitrate anions are coordinated in a biden-

Table 3 Metal–ligand bond distances (in Å) for M(TEtDAPhen)$(NO_3)_3$ complexes

Bond	1-Pr	1-Nd	1-Tb	1-Lu	1-Am
M–O1	2.477(2)	2.4745(10)	2.3617(11)	2.2856(16)	2.466(4)
M–O2	2.463(3)	2.4119(11)	2.4210(11)	2.3173(14)	2.424(4)
M–N2	2.650(3)	2.6126(12)	2.5484(12)	2.4558(15)	2.594(5)
M–N3	2.652(3)	2.6738(11)	2.6088(12)	2.4303(15)	2.655(5)
M–$O3_{(NO_3)}$	2.559(3)	2.5866(11)	2.5341(12)	2.4753(15)	2.584(5)
M–$O4_{(NO_3)}$	2.527(3)	2.5417(11)	2.4686(11)	2.3672(15)	2.554(5)
M–$O6_{(NO_3)}$	2.552(9)	2.5186(10)	2.4439(10)	2.3536(16)	2.521(4)
M–$O7_{(NO_3)}$	2.568(11)	2.5334(11)	2.4780(11)	2.3843(16)	2.542(4)
M–$O9_{(NO_3)}$	2.563(3)	2.5561(11)	2.5037(12)	2.236(9)	2.559(5)
M–$O10_{(NO_3)}$	2.549(3)	2.5308(10)	2.4676(11)	—	2.524(4)

tate fashion, and one is coordinated monodentate while the ligand coordinates in a tetradentate fashion (crystallographic Table S4†). The Lu(TEtDAPhen)$(NO_3)_3$ 9-coordinate complex was also observed in the TBuDAPhen system.[46] The Lu–O_L are 2.2856(16) and 2.3173(14) Å and the Lu–N bonds are 2.4558 (15) and 2.4303(15) Å. In comparison to the lighter lanthanides, the distortion of the Lu structure shows slight asymmetry in the bonding. The Lu–$O_{(NO_3)}$ bond lengths range from 2.236(9)–2.4753(15) Å which are comparable to the other Lu-nitrate bonds.[45]

The Lu(TEtDAPhen)$(NO_3)_3$ complex shows a new binding mode where the M–O_L bonds point above and below the plane of the phenanthroline backbone (Fig. 6). Because of this asymmetry, the Lu–O_L and the Lu–N are distorted to adjust to the small size of the metal cation. The Lu–O_L bonds oxygens extend above and below the plane of the phenanthroline backbone at 0.797 and 0.369 Å, respectively. In comparison to other structures, only the oxygens display distortion, whereas the M–N bonds remain symmetrical. As a consequence of this bonding motif, the ethyl chains are in a *cis*-conformation. This distortion has been observed in the TBuDAPhen system for the heavier lanthanides ranging from Dy(III)–Er(III). However, the butyl chains have more flexibility than the ethyl chains to compensate for the distortion caused by metal coordination.[44]

The crystallographic study of this system shows that the structure of Am(TEtDAPhen)$(NO_3)_3$ closely resembles that of early lanthanide complexes, specifically Pr(III) and Nd(III). This similarity suggests that the selectivity of TEtDAPhen for An(III) is not driven by structural factors, but rather by electronic differences. The observed symmetry in the Pr–O_L bonds, compared to the increasing asymmetry in other M–O_L bonds reported in this study, indicates a size-dependent organization of the TEtDAPhen ligand around the metal center. Additionally, the distortion of the phenanthroline backbone in the Lu(TEtDAPhen)$(NO_3)_3$ structure and the transition from a 10-coordinate to a 9-coordinate geometry suggest that TEtDAPhen is unlikely to be selective for the later Ln(III) elements.

Am(TEtDAPhen)$(NO_3)_3$ analysis

To further analyze the Am(TEtDAPhen)$(NO_3)_3$ complex, HSQC NMR and UV-Visible spectra were obtained, shown in Fig. 7 and 8. The HSQC NMR reveal a strong correlation between the ^{13}C and ^{1}H NMR peaks observed. This correlation suggests that the Am(TEtDAPhen)$(NO_3)_3$ solid state structure persists in solution.

Solution phase UV-Visible absorption spectra from Am (TEtDAPhen)$(NO_3)_3$ and the free TEtDAPhen is consistent with the NMR data and suggests that complexation of Am(III) by TEtDAPhen occurs in solution. These results reflect the Am (TEtDAPhen)$(NO_3)_3$ complex with the relatively sharp absorbance peaks at *ca.* 20 000 cm^{-1} (500 nm) and *ca.* 13 000 cm^{-1} (810 nm) that are characteristic of Am(III). Using nomenclature typical for a free Am(III) cation, we assigned these features to the Laporte forbidden 5f → 5f electronic transitions from the

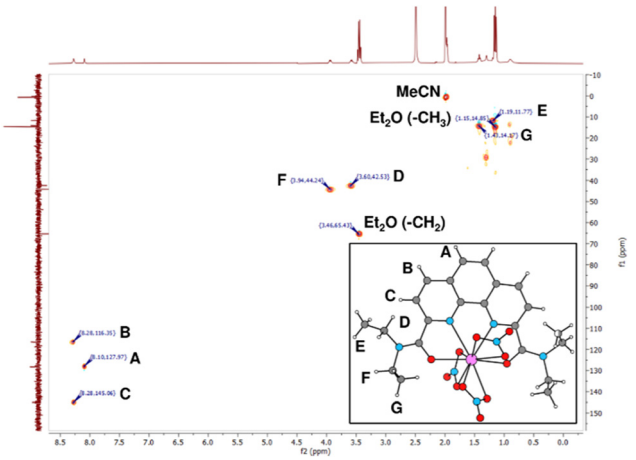

Fig. 7 HSQC NMR of the supernatant from the Am(TEtDAPhen)$(NO_3)_3$ crystallization solution in CD_3CN. The *y*-axis shows the ^{13}C DEPT NMR spectrum while the *x*-axis shows the ^{1}H NMR spectrum.

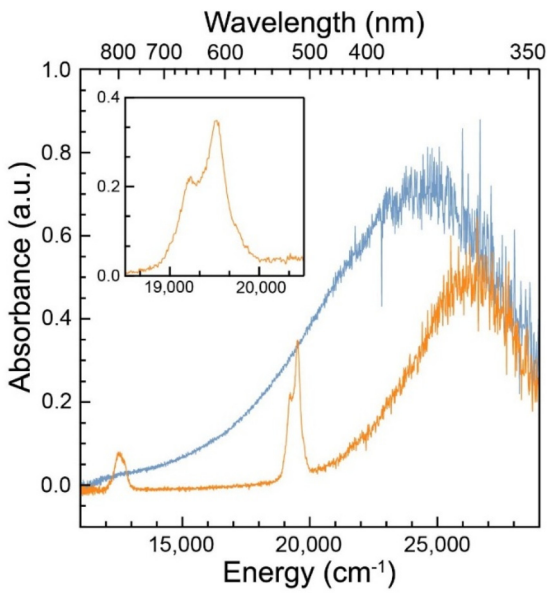

Fig. 8 UV/vis absorption spectra in CD_3CN of Am(TEtDAPhen)$(NO_3)_3$ (orange trace) and TEtDAPhen (blue trace).

$^{7}F_0$ ground state to the $^{5}L_6$ (~20 000 cm^{-1}) and $^{7}F_5$ (13 000 cm^{-1}) excited states.[12,47]

The $^{5}L_6$ transition at ~500 nm presents a shoulder peak that is red shifted from the main peak. This is an additional piece of evidence for the complexation of Am(III) to the TEtDAPhen ligand.

Conclusions

The extraction properties and coordination chemistry of TEtDAPhen with An(III) (An = Am, Cm, Bk, Cf) *vs.* Eu(III) have been studied. The TEtDAPhen extractant preferentially extracts

An(III) over Eu(III). The degree to which each An(III) was extracted did not increase as one moved across the actinide series as expected. Instead, Am(III) was extracted to the largest extent, then Bk(III) and Cf(III), and Cm(III) was extracted to the smallest extent. Although the separation factors achieved for TEtDAPhen do not match the highest reported in the DAPhen class of ligands, they demonstrate a promising level of selectivity and within the context of the comprehensive approach presented here. These findings provide a foundation for further optimization and highlight the potential of this system for An(III) separation.

To provide insight into the extraction, stability constants were determined for Ln(III) (Ln = Nd, Eu, Gd) using UV-Vis spectrophotometric titration. Those data showed an increased stability constant with decreasing ionic radii, such that the smallest and most strongly polarizing Gd(III) cation had the highest stability constant. Analysis of the UV-Vis spectrophotometric titrations suggested that in solution the Ln(III) cations formed one-to-one complexes with TEtDAPhen. Complexation studies were consistent with this formulation and Ln(TEtDAPhen)$(NO_3)_3$ complexes were independently synthesized and characterized by single crystal X-ray diffraction. Interestingly, it was found that the same structure type was obtained for Am(III) as Am(TEtDAPhen)$(NO_3)_3$, which was fully characterized using UV-Visible spectroscopy, ^{1}H and ^{13}C NMR spectroscopy, and by single crystal X-ray diffraction (see ESI† for spectra). Comparative analyses of the Am(TEtDAPhen)$(NO_3)_3$ and Ln(TEtDAPhen)$(NO_3)_3$ structures showed subtle differences. Further, the metal–ligand distances and angles systematically varied as the ionic radius of the central metal cation decreased. It is speculated the origin for these distortions reflect the flexibility of the ligand environment that minimizes unfavorable steric crowding between the TEtDAPhen and NO_3^- ligands for Lu(III) *versus* Pr(III). It is intriguing that there is no obvious structural feature highlighting the selectivity of TEtDAPhen for Am(III) over Ln(III) cations. Perhaps there is an electronic structure difference between Am(TEtDAPhen)$(NO_3)_3$ and Ln(TEtDAPhen)$(NO_3)_3$ responsible for this divergent affinity. As a result of this speculation, more analysis is required to validate this conclusion. At this point, these results can be used as motivation for more detailed physical characterization of the M(TEtDAPhen)$(NO_3)_3$ complexes and as an impetus to conduct calculations and comparatively evaluate An- *versus* Ln-(TEtDAPhen)$(NO_3)_3$ bonding interactions.

Experiments

Chemical reagents

Neocuproine hydrate (99%), selenium dioxide (ReagentPlus®, powder, 99.8% trace metals basis), 1,4-dioxane (ACS reagent, ≥99.0%), thionyl chloride (reagent grade, >97%), triethylamine (≥99.5%), diethylamine (≥99.5%), and nitrobenzene (ACS reagent, ≥99.0%) were purchased from Sigma-Aldrich and used as received. Nitric acid (OmniTrace®, 67–70%) used in this study was obtained from Millipore. Dichloromethane (certified ACS), diethyl ether (anhydrous, ACS Grade), hexanes (certified ACS), and acetonitrile (Optima® LC/MS) were purchased from Fisher Chemical. The TEtDAPhen extractant was synthesized according to a previous procedure.[26]

Caution! $Eu^{152/154}$ ($t_{1/2}$ = 13/8 y), ^{241}Am ($t_{1/2}$ = 432 y), ^{243}Am ($t_{1/2}$ = 7364 y), ^{244}Cm ($t_{1/2}$ = 18 y), ^{249}Bk ($t_{1/2}$ = 330 d), and ^{249}Cf ($t_{1/2}$ = 351 y) represent serious health risks due to the α, β and γ emissions of these radioisotopes and their daughters. All studies were conducted in laboratories dedicated to transuranic element research equipped with HEPA filtered hoods, continuous air monitors and proper dosimetry for personnel. Stock solutions of ^{241}Am in (HNO_3, 1 M; Eckert and Ziegler), ^{244}Cm (HNO_3, 0.01 M; Eckert and Ziegler), ^{249}Bk (HNO_3, 0.01 M; Oak Ridge National Laboratory), and ^{249}Cf ($HClO_4$, 0.01 M; prepared and purified at Florida State University) were used as received. The ^{243}Am radionuclide was obtained from the National Isotope Production Program. The ^{243}Am was subsequently recovered and purified using a previously published procedure prior to use because this sample had been used in previous research campaigns.[48,49] That procedure generated an $^{243}Am^{3+}_{(aq)}$ stock solution that was 6.75 mM in Am^{3+} and in 6 M in $HCl_{(aq)}$. A solution of $^{152/154}$Eu in 0.01 M HNO_3 was made using the United States Geological Survey (USGS) TRIGA reactor by irradiating a solution of $Eu(NO_3)_3$ dissolved in 1 M HNO_3. Nd_2O_3 (Treibacher Industries AG), Lu_2O_3 (Treibacher Industries AG), $Pr(NO_3)_3{\cdot}6(H_2O)$ (Alpha Aesar), and $Tb(NO_3){\cdot}6(H_2O)$ (99.99%, Alfa Aesar) were purchased and used as received.

Solvent extraction

The solvent extraction measurements were performed at room temperature, with equal phase ratio, and in triplicate. The TEtDAPhen extractant was dissolved in nitrobenzene at various concentrations (0.05–0.2 M). The TEtDAPhen solutions were pre-equilibrated with three $HNO_{3(aq)}$ solutions (either 1, 3, or 5 M). The organic and aqueous phases were contacted using a shaker table (60 minutes at 2000 rpm), centrifuged (2800 rpm for 5 minutes) and the aqueous phase was discarded. The organic phase was then contacted with a fresh aqueous phase (either 1, 3 or 5 M HNO_3) of equal volume (0.5 mL). After, radioactive tracers (μM [M^{3+}]) were added to the vial with enough volume to provide 10 000 cpm, 8000 cpm, 9000 dpm, 10 000 dpm, and 13 000 cpm for $^{152/154}$Eu, ^{241}Am, ^{244}Cm, ^{249}Bk, and ^{249}Cf, respectively. The samples were shaken (60 minutes at 2000 rpm), centrifuged (2800 rpm for 5 minutes), and then an aliquot was pulled for assay from each phase. The aliquot size was 200 μL for the Eu(III), Am(III), and Cf(III) experiments and 100 μL for the Cm(III) and Bk(III) experiments. The $^{152/154}$Eu, ^{241}Am, and ^{249}Cf aliquots were assayed by γ-spectrometry on a Packard COBRA II with data acquisition windows of 40–225 keV, 40–100 keV, and 200–410 keV, respectively. The ^{244}Cm and ^{249}Bk samples were counted on a HIDEX 300 SL with data acquisition windows of 0–1023 and 0–550, respectively. The LSC HIDEX 300 SL samples were prepared by adding the aliquot to 5 or 7 mL of Ultima Gold AB.

The distribution ratio, D, was calculated for $^{152/154}$Eu, ^{241}Am, ^{249}Cf, and ^{244}Cm using the ratio of the radiometrically counted activity in the organic phase to the counts in the aqueous phase. For ^{249}Bk, the D was calculated using eqn (2) where A_i is the initial count value in the aqueous phase before extraction and A_f is the final count value in the aqueous phase post-extraction in response to significant quenching caused by beta particle energy transfer in the LSC cocktail in response to nitrobenzene in the organic phase samples. Mass balance was ensured upon stripping the radioactivity from the organic phase. This was done by contacting the organic phase with 0.01 M HNO_3 in a one-to-three organic : aqueous ratio three times to confirm all activity was stripped from the organic phase. The separation factors, SF, were calculated using a ratio of D values.

$$D = \frac{A_i - A_f}{A_f} \quad (2)$$

UV-Visible spectroscopy

UV-Vis-NIR spectroscopy was carried out on a Varian Cary300 at room temperature. A 0.02 mM solution of TEtDAPhen was prepared by dissolving TEtDAPhen in methanol. Meanwhile, 0.45 mM solutions of $Nd(NO_3)_3{\cdot}6H_2O$, $Eu(NO_3)_3{\cdot}6H_2O$, $Gd(NO_3)_3{\cdot}6H_2O$ were prepared in methanol from stock solutions of $Nd(NO_3)_3{\cdot}6H_2O$ (0.548 M), $Eu(NO_3)_3{\cdot}6H_2O$ (0.534 M), and $Gd(NO_3)_3{\cdot}6H_2O$ (0.497 M). An aliquot of the 0.02 mM TEtDAPhen solution was transferred to a quartz cuvette (1 cm pathlength) and assayed by UV-Vis spectroscopy. Subsequently, a small aliquot (5 μL) of the metal solution was added to the cuvette and the solution was mixed by inversion repeatedly to ensure homogeneity. This act was repeated 25 times per metal solution, which transferred a total of 125 μL of each metal solution to the cuvette in each titration case. Note, at the end of the titration a total of 2 $M(NO_3)_3$ equivalents were added to one equivalent of TEtDAPhen. All UV-Vis measurements were made from 240–380 nm with a scan rate of 600 nm min^{-1} and interval of 1 nm. Data acquisition persisted until no change occurred in the spectral features. Stability constants and factor analysis were calculated and obtained in HypSpec2014 accounting for dilution of the metal and ligand solutions.

Synthetic procedures

Synthesis of *N*,*N*,*N*′,*N*′-tetraethyl-2,9-diamide-1,10-phenanthroline americium(III) trinitrate; Am(TEtDAPhen)$(NO_3)_3$. In a fume hood and with no attempt to exclude air and moisture, an aliquot (1.22 mL) from the $^{243}Am^{3+}_{(aq)}$ stock solution (6.75 mM ^{243}Am, in 6 M in HCl) was pipetted into a Pyrex® glass Falcon cone (50 mL). Hence the total amount of Am^{3+} transferred to the cone was 2.00 mg (8.23 μmol). The flask was gently heated on a hot plate (70 °C) until the solution evaporated and a soft-dryness was achieved. The term "soft dryness" was used to warn the reader about prologued heating during the evaporation process, which can bake the residue to the beaker and complicate subsequent dissolution efforts. The resulting residue was dissolved in $HNO_{3(aq)}$ (approx. 2 mL; concentrated, approx. 16 M; Optima® grade). The Falcon cone was gently heated on a hot plate (70 °C) until the solution evaporated and a soft-dryness was achieved. The resulting residue was dissolved again in $HNO_{3(aq)}$ (approx. 2 mL; concentrated, approx. 16 M; Optima® grade) and heated until the water evaporated. To ensure complete removal of Cl^-, this evaporation and dissolution step was repeated a total of three times, in that $HNO_{3(aq)}$ was added a total of three times. This left an americium-containing residue that formulated as a hydrated americium nitrate salt of the general formula $[Am(H_2O)_y(NO_3)_x][NO_3]_{3-x}{\cdot}zH_2O$. This residue readily dissolved in MeCN (500 μL). That pink solution was transferred to a Pyrex vial (1 dram). Separately, a Pyrex vial (1 dram) was charged with TEtDAPhen (3.7 mg, 0.01 mmol). This brown powder dissolved in MeCN (250 μL) to generate a deep orange-brown solution. Adding this solution to the vial that contained $[Am(H_2O)_y(NO_3)_x][NO_3]_{3-x}{\cdot}zH_2O$ caused the americium nitrate to dissolve and generated an orange-brown solution. This reaction vial was placed in a scintillation vial (20 mL) that contained diethyl ether (1 mL). The scintillation vial was capped and block-like orange crystals of Am(TEtDAPhen)$(NO_3)_3$ formed overnight as the diethyl ether antisolvent slowly diffused into the MeCN solution. Some of these crystals were suitable for single crystal X-ray diffraction. The crystal yield is estimated to be 50% based on analogous scoping experiments carried out with Nd((III)) that were used to benchmark this procedure. Since all crystals of Am(TEtDAPhen)$(NO_3)_3$ were consumed during the XRD experiment, the supernatant of the crystallization was used to acquire NMR spectra. The supernatant was transferred to a glass 1 dram vial and allowed to evaporate in a HEPA filtered fume hood overnight to dryness. The leftover residue was then redissolved in ~2 mL of CD_3CN (Sigma-Aldrich, ≥99.8 atom % D). The NMR sample was prepared using a triple-containment procedure outlined elsewhere.[50] Interpretation of the NMR spectrum was facilitated by HMQC experiments. ^{1}H NMR (400 MHz, CD_3CN): δ 8.28 (q, 2H), 8.10 (s, 1H), 3.94 (q, 2H), 3.46 (q, 2H), 1.43 (t, n/a), 1.19 (t, n/a). ^{13}C NMR (400 MHz, CD_3CN): δ 145.06, 127.97, 116.35, 44.24, 42.53, 14.17, 11.77. UV-Vis: 377 nm, 512 nm, 796 nm.

Am(TEtDAPhen)$(NO_3)_3$. The sample used to acquire the NMR data described in the "Synthesis of *N*,*N*,*N*′,*N*′-tetraethyl-2,9-diamide-1,10-phenanthroline americium(III) trinitrate; Am(TEtDAPhen)$(NO_3)_3$" section was also used for the UV-vis absorption studies. Absorption measurements were acquired on a StellarNet spectrometer with blue-wave and red-wave DS-InGaAs-512 detectors. The cuvette holder was housed in a HEPA filtered fume hood and connected to the spectrometer with fiber optic cables. A spectrum of TEtDAPhen was also acquired on a 2.91 mM solution prepared by dissolving 2.2 mg of TEtDAPhen in 1 mL of CD_3CN. 300 μL of the resulting solution was then diluted in 300 μL of CD_3CN, resulting a final concentration of 2.91 mM. UV-vis measurements were acquired from 195–1044 nm (see Fig. 8).

Synthesis of *N*,*N*,*N*′,*N*′-tetraethyl-2,9-diamide-1,10-phenanthroline lanthanide(III) trinitrate; Ln(TEtDAPhen)$(NO_3)_3$

Synthesis of Nd(TEtDAPhen)(NO$_3$)$_3$. In a fume hood with no attempt to exclude air and moisture, a beaker was charged with Nd_2O_3. The solid was dissolved in a minimum amount of $HNO_{3(aq)}$. The resulting blue/purple solution was heated on a hot plate until the solution evaporated completely. This process was performed three times to obtain $Nd(NO_3)_3{\cdot}6H_2O$. A 1-dram vial was charged with the $Nd(NO_3)_3{\cdot}6H_2O$ species (6.5 mg, 0.015 mmol) of the purple residue left after the evaporation was transferred to a 1-dram vial and dissolved in MeCN (0.5 mL). Meanwhile, a separate 1-dram vial was charged with TEtDAPhen (6.17 mg, 0.018 mmol) and dissolved in MeCN (0.5 mL) to make a lightly brown solution. This solution was added to the neodymium containing flask. The reaction flask was placed in a scintillation vial (20 mL) that contained diethyl ether (3 mL) and was allowed to vapor diffuse overnight to form suitable crystals for X-ray diffraction. The vial was capped, and crystals formed overnight. The mother liquor was removed by decantation, the crystals dried under vacuum, and the complex was isolated. Some of these crystals were suitable for single crystal X-ray diffraction (50% yield). ^{1}H NMR (500 MHz, CD_3CN): δ 11.60 (s, 1H), 10.58 (s, 1H), 9.24 (s, 1H), 8.24 (s, 2H), 5.89 (s, 2H), 3.54 (s, 3H), 2.77 (s, 3H), 1.20 (s, 1H). Elemental analysis for $C_{22}H_{26}N_7O_{11}Nd$: calculated C, 37.28; H, 3.70; N, 13.83. Found C, 38.43; H, 4.12; N, 12.23. UV-Vis: 295 nm, 237 nm, 207 nm. IR: 1594 cm^{-1}, 1460 cm^{-1}, 1277 cm^{-1}, 1029 cm^{-1}, 713 cm^{-1}.

Synthesis of Lu(TEtDAPhen)(NO$_3$)$_3$. The procedure written above was repeated for Lu_2O_3. For the crystallization, 5.7 mg (0.012 mmol) was used (15% yield). ^{1}H NMR (500 MHz, CD_3CN): δ 8.46 (d, 2H), 7.93 (d, 2H), 7.83 (s, 2H), 3.50 (m, 4H), 3.28 (m, 4H), 1.49 (m, 2H), 1.10 (t, 6H), 0.90 (t, 6H). Elemental analysis for $C_{22}H_{26}N_7O_{11}Lu$: calculated C, 35.73; H, 3.54; N, 13.26. Found C, 36.64; H, 4.35; N, 11.64. UV-Vis: 297 nm, 240 nm, 209 nm. IR: 1600 cm^{-1}, 1465 cm^{-1}, 1290 cm^{-1}, 1029 cm^{-1}, 712 cm^{-1}.

Synthesis of Pr(TEtDAPhen)(NO$_3$)$_3$ and Tb(TEtDAPhen)(NO$_3$)$_3$. $Pr(NO_3)_3{\cdot}6H_2O$ (6.5 mg, 0.015 mmol) (50% yield) and $Tb(NO_3)_3{\cdot}5H_2O$ (6.8 mg, 0.016 mmol) (50% yield) were used directly and followed the same crystallization procedure as written above.

Pr(TEtDAPhen)(NO$_3$)$_3$. NMR (500 MHz, CD_3CN): δ 13.01 (s, 1H), 11.69 (s, 2H), 10.93 (s, 1H), 8.97 (s, 1H), 7.09 (s, 2H), 5.40 (s, 3H), 3.76 (s, 3H), 1.25 (s, 1H). Elemental analysis for $C_{22}H_{26}N_7O_{11}$: calculated C, 37.28; H, 3.70; N, 13.83. Found C, 38.78; H, 4.29; N, 11.96. UV-Vis: 297 nm, 240 nm, 209 nm. IR: 1600 cm^{-1}, 1458 cm^{-1}, 1303 cm^{-1}, 1260 cm^{-1}, 879 cm^{-1}, 717 cm^{-1}.

Tb(TEtDAPhen)(NO$_3$)$_3$. NMR: due to paramagnetism, NMR was not obtainable. Elemental analysis for $C_{22}H_{26}N_7O_{11}Tb$: calculated C, 36.53; H, 3.62; N, 13.55. Found C, 36.88; H, 4.02; N, 12.76. UV-Vis: 295 nm, 234 nm, 208 nm. IR: 1597 cm^{-1}, 1462 cm^{-1}, 1287 cm^{-1}, 1032 cm^{-1}, 712 cm^{-1}.

X-Ray crystallography

Single crystals of Am(TEtDAPhen)(NO$_3$)$_3$ suitable for X-ray diffraction were obtained as described in the "Synthesis of 2,9-diamide-1,10-phenanthroline americium(III) trinitrate; Am(TEtDAPhen)(NO$_3$)$_3$" section. These crystals were submerged in mineral oil and mounted on a MiTeGen Micromount™. Multiple layers of containment were employed to encapsulate the americium crystals and guard against the spread of unwanted contamination using a previously published procedure.[51] This encapsulation method involved encasing the crystal in epoxy, gluing the crystal to the mounting loop, and sliding the loop into a plastic sheath that was sealed to the crystal mount with epoxy. Low temperature (100 K) X-ray diffraction data were collected using a Bruker D8 Quest equipped with a CPAD Photon II™ area detector and a MoK_α IμS 3.0 micro source™. APEX 3 software was used for data collection and initial unit cell indexing and refinement. The structure was solved using the Olex2 software package and SHELXT structure solution program by Intrinsic Phasing.[52–54] A multi-scan was used for an absorption correction. The structural refinement was performed using SHELXL within the ShelXle software interface. See the ESI† for a table that contains crystallographic parameters. Figures were produced using VESTA and Olex2.[52,55]

All non-hydrogen atoms were located in the Fourier difference map and refined anisotropically. This generated a structural model that consisted of a Am(III) bound to one TEtDAPhen and three NO_3^- ligands per asymmetric unit. Hydrogen atoms were placed in calculated positions and their U_{eq} values were assigned values 1.2 times that of their parent atom.

Single crystals M(TEtDAPhen)(NO$_3$)$_3$ (M: Pr, Nd, Tb, Lu) were mounted on a MiTeGen Micromount™ with Krytox oil, and the crystals were optically aligned on a Bruker D8 Quest X-ray diffractometer using a built-in camera. Preliminary measurements were performed using an I-μ-S X-ray source (Mo Kα, λ = 0.71073 Å) with high-brilliance and high-performance focusing quest multilayer optics. Data were collected at 100 K using an Oxford cryosystems crystream 1000, reflections were indexed and processed, and the files were scaled and corrected for absorption using APEX2. The reflection's intensities of a sphere were collected by a mixture of four sets of frames. Each set had a different omega angle for the crystal, and each exposure covered a range of 0.50 in ω, totalling 1464 frames. The frames were collected with an exposure time of 5–25 which was dependent on the crystal. SAINT software was used for data integration including polarization and Lorentz corrections. The files were scaled and corrected for absorption using SADABS. The space groups were assigned, and the structures were solved by direct methods using XPREP within the SHELXTL suite of programs.

Author contributions

Emma M. Archer, Shane S. Galley, and Jenifer C. Shafer conceived the study. Emma M. Archer wrote the original draft of the paper. All authors contributed to revising the

manuscript. Emma M. Archer completed and analyzed the solvent extraction and UV-Visible titration data. Emma M. Archer, Jocelyn M. Riley, Elizabeth B. Flynn, and Shane S. Galley contributed ligand synthesis and purification in addition to crystal growth and preparation. Jacob P. Brannon collected, and Shane S. Galley analyzed the crystallographic data. The LANL authors contributed to synthesis and characterization of the americium complex. This included Am(III) purification, sample preparation, single crystal X-ray absorption measurements, analysis by UV-Visible spectrum, and NMR.

Conflicts of interest

There are no conflicts to declare.

Data availability

Crystallographic data for the structures reported in this manuscript have been deposited at the Cambridge Structural Database.[56] The deposition numbers are (Am) 2385181, (Pr) 2385184, (Nd) 2385185, (Tb) 2385183, and (Lu) 2385182.† The data for the reported structures in this manuscript can be obtained at **https://www.ccdc.cam.ac.uk/structures/**. Additional data can be found in the ESI.†

Acknowledgements

This work was supported by the U.S. Department of Energy Office of Science, Office of Basic Energy Sciences, and Colorado School of Mines under award number DE-SC0020189 (E. M. A., S. S. G., J. A. J., and J. C. S.). We thank the U.S. Department of Energy, Office of Science, Office of Basic Energy Sciences, Heavy Element Chemistry program (2020LANLE372) (J. C. G.; B. L. H.; J. G. K; S. A. K.) and the US Department of Energy, National Nuclear Security Association (NNSA), Plutonium Modernization Program (NA-191; B. N. L.) for funding the synthesis and characterization of Am(TEtDAPhen)$(NO_3)_3$ complex. Additional support for this effort came from LANL's LDRD projects (20220054DR) for characterization measurements. We thank the Glenn T. Seaborg Institute (Gilhula), and the US Department of Energy, National Nuclear Security Association (NNSA), Plutonium Modernization Program (NA-191). The ^{243}Am radionuclide used in this research was supplied by the U.S. Department of Energy Isotope Program, managed by the Office of Isotope R&D and Production. For student support, we thank the U.S. D.O.E. through a University Nuclear Leadership Program graduate fellowship (F. A. P.). LANL is an affirmative action/equal opportunity employer managed by Triad National Security, LLC, for the National Nuclear Security Administration of the U.S. DOE. LA-UR-24-23890.

References

1 I. Petruška, E. Litavcová and J. Chovancová, Impact of Renewable Energy Sources and Nuclear Energy on CO2 Emissions Reductions—The Case of the EU Countries, *Energies*, 2022, **15**(24), 1–23, DOI: **10.3390/en15249563**.
2 J. Veliscek-Carolan, Separation of Actinides from Spent Nuclear Fuel: A Review, *J. Hazard. Mater.*, 2016, **318**, 266–281.
3 W. B. Lanham and T. C. Runion, *PUREX Process for Plutonium and Uranium Recovery*, Oak Ridge, 1949.
4 A. Bhattacharyya and P. K. Mohapatra, Separation of Trivalent Actinides and Lanthanides Using Various "N", "S" and Mixed "N,O" Donor Ligands: A Review, *Radiochim. Acta*, 2019, **107**, 931–949.
5 P. J. Panak and A. Geist, Complexation and Extraction of Trivalent Actinides and Lanthanides by Triazinylpyridine N-Donor Ligands, *Chem. Rev.*, 2013, **113**(2), 1199–1236.
6 K. L. Nash, A Review of the Basic Chemistry and Recent Developments in Trivalent F-Element Separations, *Solvent Extr. Ion Exch.*, 1993, **11**(4), 729–768.
7 T. Kooyman, Current State of Partitioning and Transmutation Studies for Advanced Nuclear Fuel Cycles, *Ann. Nucl. Energy*, 2021, **157**, 108239.
8 G. J. Lumetta, D. Neiner, S. I. Sinkov, J. C. Carter, J. C. Braley, S. L. Latesky, A. V. Gelis, P. Tkac and G. F. Vandegrift, Combining Neutral and Acidic Extractants for Recovering Transuranic Elements from Nuclear Fuel. In 19th International Solvent Extraction Conference, Santiago, 2011.
9 M. P. Kelley, N. P. Bessen, J. Su, M. Urban, S. I. Sinkov, G. J. Lumetta, E. R. Batista, P. Yang and J. C. Shafer, Revisiting Complexation Thermodynamics of Transplutonium Elements up to Einsteinium, *Chem. Commun.*, 2018, **54**(75), 10578–10581.
10 A. E. Clark, P. Yang and J. C. Shafer, Coordination of Actinides and the Chemistry behind Solvent Extraction, in *Experimental and Theoretical Approaches to Actinide Chemistry*, 2018, pp. 237–282.
11 M. P. Kelley, J. Su, M. Urban, M. Luckey, E. R. Batista, P. Yang and J. C. Shafer, On the Origin of Covalent Bonding in Heavy Actinides, *J. Am. Chem. Soc.*, 2017, **139**(29), 9901–9908.
12 S. K. Cary, J. Su, S. S. Galley, T. E. Albrecht-Schmitt, E. R. Batista, M. G. Ferrier, S. A. Kozimor, V. Mocko, B. L. Scott, C. E. Van Alstine, F. D. White and P. Yang, A Series of Dithiocarbamates for Americium, Curium, and Californium, *Dalton Trans.*, 2018, **47**(41), 14452–14461.
13 M. J. Hudson, L. M. Harwood, D. M. Laventine and F. W. Lewis, Use of Soft Heterocyclic N-Donor Ligands to Separate Actinides and Lanthanides, *Inorg. Chem.*, 2013, **52**(7), 3414–3428.
14 V. A. Babain, M. Y. Alyapyshev and L. I. Tkachenko, ACTINIDE-LANTHANIDE SEPARATION WITH SOLVENTS ON THE BASE OF AMIDES OF HETERCYCLIC DIACIDS, in *Global 2013*, 2013, pp. 1486–1489.

15 M. Y. Alyapyshev, V. A. Babain and L. I. Tkachenko, Amides of Heterocyclic Carboxylic Acids as Novel Extractants for High-Level Waste Treatment, *Radiochemistry*, 2014, **56**(6), 565–574.
16 M. V. Evsiunina, P. I. Matveev, S. N. Kalmykov and V. G. Petrov, Solvent Extraction Systems for Separation of An(III) and Ln(III): Overview of Static and Dynamic Tests, *Moscow Univ. Chem. Bull.*, 2021, **76**(5), 287–315.
17 A. Leoncini, J. Huskens and W. Verboom, Ligands for F-Element Extraction Used in the Nuclear Fuel Cycle, *Chem. Soc. Rev.*, 2017, **46**(23), 7229–7273.
18 R. G. Pearson, Hard and Soft Acids and Bases, *J. Am. Chem. Soc.*, 1963, **85**(22), 3533–3539.
19 F. W. Lewis, L. M. Harwood, M. J. Hudson, M. G. B. Drew, V. Hubscher-Bruder, V. Videva, F. Arnaud-Neu, K. Stamberg and S. Vyas, BTBPs versus BTPhens: Some Reasons for Their Differences in Properties Concerning the Partitioning of Minor Actinides and the Advantages of BTPhens, *Inorg. Chem.*, 2013, **52**(9), 4993–5005.
20 F. W. Lewis, L. M. Harwood, M. J. Hudson, M. G. B. Drew, A. Wilden, M. Sypula, G. Modolo, T.-H. Vu, J.-P. Simonin, G. Vidick, N. Bouslimani and J. F. Desreux, From BTBPs to BTPhens: The Effect of Ligand Pre-Organization on the Extraction Properties of Quadridentate Bis-Triazine Ligands, *Procedia Chem.*, 2012, **7**, 231–238.
21 E. M. Archer, S. S. Galley, J. A. Jackson and J. C. Shafer, Investigation of f-Element Interactions with Functionalized Diamides of Phenanthroline-Based Ligands, *Solvent Extr. Ion Exch.*, 2023, **41**(6), 697–740.
22 L. Xu, X. Yang, A. Zhang, C. Xu and C. Xiao, Separation and Complexation of F-Block Elements Using Hard-Soft Donors Combined Phenanthroline Extractants, *Coord. Chem. Rev.*, 2023, **496**, 215404.
23 P. Ren, P. W. Huang, X. F. Yang, Y. Zou, W. Q. Tao, S. L. Yang, Y. H. Liu, Q. Y. Wu, L. Y. Yuan, Z. F. Chai and W. Q. Shi, Hydrophilic Sulfonated 2,9-Diamide-1,10-Phenanthroline Endowed with a Highly Effective Ligand for Separation of Americium(III) from Europium(III): Extraction, Spectroscopy, and Density Functional Theory Calculations, *Inorg. Chem.*, 2021, **60**(1), 357–365.
24 X.-F. Yang, Y. Liu, W.-Q. Tao, S. Wang, P. Ren, S.-L. Yang, L.-Y. Yuan, H.-B. Tang, Z.-F. Chai and W.-Q. Shi, Lipophilic Phenanthroline Diamide Ligands in 1-Octanol for Separation of Am(III) from Eu(III), *J. Environ. Chem. Eng.*, 2022, **10**, 1–12.
25 X. Yang, L. Xu, D. Fang, A. Zhang and C. Xiao, Progress in Phenanthroline-Derived Extractants for Trivalent Actinides and Lanthanides Separation: Where to Next?, *Chem. Commun.*, 2024, **60**(81), 11373–11598.
26 X. Zhang, L. Yuan, Z. Chai and W. Shi, Towards Understanding the Correlation between UO22+ Extraction and Substitute Groups in 2,9-Diamide-1,10-Phenanthroline, *Sci. China: Chem.*, 2018, **61**(10), 1285–1292.
27 Y. Li, X. Yang, P. Ren, T. Sun, W. Shi, J. Wang, J. Chen and C. Xu, Substituent Effect on the Selective Separation and Complexation of Trivalent Americium and Lanthanides by N,O-Hybrid 2,9-Diamide-1,10-Phenanthroline Ligands in Ionic Liquid, *Inorg. Chem.*, 2021, **60**(7), 5131–5139.
28 X. Zhang, X. Kong, L. Yuan, Z. Chai and W. Shi, Coordination of Eu(III) with 1,10-Phenanthroline-2,9-Dicarboxamide Derivatives: A Combined Study by MS, TRLIF, and DFT, *Inorg. Chem.*, 2019, **58**(15), 10239–10247.
29 S. Wang, X. Yang, Y. Liu, L. Xu, C. Xu and C. Xiao, Enhancing the Selectivity of Trivalent Actinide over Lanthanide Using Asymmetrical Phenanthroline Diamide Ligands, *Inorg. Chem.*, 2024, **63**(6), 3063–3074.
30 A. M. Wilson, P. J. Bailey, P. A. Tasker, J. R. Turkington, R. A. Grant and J. B. Love, Solvent Extraction: The Coordination Chemistry behind Extractive Metallurgy, *Chem. Soc. Rev.*, 2014, **43**(1), 123–134.
31 M. Laing, Solvent Extraction of Metals Is Coordination Chemistry, in *ACS Symposium Series*, UTC, 1994, vol. 16, pp. 382–394.
32 N. Tsutsui, Y. Ban, H. Suzuki, M. Nakase, S. Ito, Y. Inaba, T. Matsumura and K. Takeshita, Effects of Diluents on the Separation of Minor Actinides from Lanthanides with Tetradodecyl-1,10-Phenanthroline-2,9-Diamide from Nitric Acid Medium, *Anal. Sci.*, 2020, **36**(2), 241–246.
33 X. Zhang, Q. Wu, J. Lan, L. Yuan, C. Xu, Z. Chai and W. Shi, Highly Selective Extraction of Pu(IV)and Am(III)by N, N″-Diethyl-N,N″-Ditolyl-2,9-Diamide-1,10-Phenanthroline Ligand: An Experimental and Theoretical Study, *Sep. Purif. Technol.*, 2019, **223**, 274–281.
34 C. L. Xiao, C. Z. Wang, L. Y. Yuan, B. Li, H. He, S. Wang, Y. L. Zhao, Z. F. Chai and W. Q. Shi, Excellent Selectivity for Actinides with a Tetradentate 2,9-Diamide-1,10-Phenanthroline Ligand in Highly Acidic Solution: A Hard-Soft Donor Combined Strategy, *Inorg. Chem.*, 2014, **53**(3), 1712–1720.
35 M. Alyapyshev, J. Ashina, D. Dar'In, E. Kenf, D. Kirsanov, L. Tkachenko, A. Legin, G. Starova and V. Babain, 1,10-Phenanthroline-2,9-Dicarboxamides as Ligands for Separation and Sensing of Hazardous Metals, *RSC Adv.*, 2016, **6**(73), 68642–68652.
36 M. Alyapyshev, V. Babain, L. Tkachenko, E. Kenf, I. Voronaev, D. Dar'in, P. Matveev, V. Petrov, S. Kalmykov and Y. Ustynyuk, Extraction of Actinides with Heterocyclic Dicarboxamides, *J. Radioanal. Nucl. Chem.*, 2018, **316**(2), 419–428.
37 D. Manna, S. Mula, A. Bhattacharyya, S. Chattopadhyay and T. K. Ghanty, Actinide Selectivity of 1,10-Phenanthroline-2,9-Dicarboxamide and Its Derivatives: A Theoretical Prediction Followed by Experimental Validation, *Dalton Trans.*, 2014, **44**(3), 1332–1340.
38 R. Meng, L. Xu, X. Yang, M. Sun, C. Xu, N. E. Borisova, X. Zhang, L. Lei and C. Xiao, Influence of a N-Heterocyclic Core on the Binding Capability of N,O-Hybrid Diamide Ligands toward Trivalent Lanthanides and Actinides, *Inorg. Chem.*, 2021, **60**(12), 8754–8764.
39 P. S. Lemport, M. V. Evsiunina, P. I. Matveev, V. S. Petrov, A. S. Pozdeev, E. K. Khult, Y. V. Nelyubina,

K. L. Isakovskaya, V. A. Roznyatovsky, I. P. Gloriozov, B. N. Tarasevich, A. S. Aldoshin, V. G. Petrov, S. N. Kalmykov, Y. A. Ustynyuk and V. G. Nenajdenko, 2-Methylpyrrolidine Derived 1,10-Phenanthroline-2,9-Diamides: Promising Extractants for Am(III)/Ln(III) Separation, *Inorg. Chem. Front.*, 2022, **9**(17), 4402–4412.

40 P. Gans, A. Sabatini and A. Vacca, Determination of Equilibrium Constants from Spectrophotometric Data Obtained from Solutions of Known PH - the Program PHab, *Ann. Chim.*, 1999, **89**, 45–49.

41 P. Gans, A. Sabatini and A. Vacca, Investivation of Equilibria in Solution. Determination of Equilibrium Constants with the HYPERQUAD Suite of Programs, *Talanta*, 1996, **43**, 1739–1753.

42 B. Chen, J. Liu, L. Lv, L. Yang, S. Luo, Y. Yang and S. Peng, Complexation of Lanthanides with N, N, N′, N′-Tetramethylamide Derivatives of Bipyridinedicarboxylic Acid and Phenanthrolinedicarboxylic Acid: Thermodynamics and Coordination Modes, *Inorg. Chem.*, 2019, **58**(11), 7416–7425.

43 Y. A. Ustynyuk, P. S. Lemport, V. A. Roznyatovsky, K. A. Lyssenko, A. O. Gudovannyy, P. I. Matveev, E. K. Khult, M. V. Evsiunina, V. G. Petrov, I. P. Gloriozov, A. S. Pozdeev, V. S. Petrov, N. A. Avagyan, A. S. Aldoshin and S. N. Kalmykov, First Trifluoromethylated Phenanthrolinediamides: Synthesis, Structure, Stereodynamics and Complexation with Ln(III), *Molecules*, 2022, **27**(10), 1–18.

44 A. V. Yatsenko, M. V. Evsiunina, Y. V. Nelyubina, K. L. Isakovskaya, P. S. Lemport, P. I. Matveev, V. G. Petrov, V. A. Tafeenko, A. S. Aldoshin, Y. A. Ustynyuk and V. G. Nenajdenko, Unusual Lanthanoid Contraction in Crystal Structures of 1,10-Phenanthroline-2,9-Diamides Complexes with Lanthanoid and Yttrium Trinitrates and the Effect of Chlorine Substituents, *Polyhedron*, 2023, **243**, 2–15.

45 B. Ahrens, S. A. Cotton, N. Feeder, O. E. Noy, P. R. Raithby and S. J. Teat, Structural Variety in Nitrate Complexes of the Heavy Lanthanides with 2,2′:6′,2″-Terpyridine, and Stereoselective Replacement of Nitrate, *J. Chem. Soc., Dalton Trans.*, 2002, (no. 9), 2027–2030.

46 P. S. Lemport, M. V. Evsiunina, Y. V. Nelyubina, K. L. Isakovskaya, V. N. Khrustalev, V. S. Petrov, A. S. Pozdeev, P. I. Matveev, Y. A. Ustynyuk and V. G. Nenajdenko, Significant Impact of Lanthanide Contraction on the Structure of the Phenanthroline Complexes, *Mendeleev Commun.*, 2021, **31**, 853–855.

47 G. Tian and D. K. Shuh, A Spectrophotometric Study of Am (Iii) Complexation with Nitrate in Aqueous Solution at Elevated Temperatures, *J. Chem. Soc., Dalton Trans.*, 2014, **43**(39), 14565–14569.

48 Z. R. Jones, M. Y. Livshits, F. D. White, E. Dalodière, M. G. Ferrier, L. M. Lilley, K. E. Knope, S. A. Kozimor, V. Mocko, B. L. Scott, B. W. Stein, J. N. Wacker and D. H. Woen, Advancing Understanding of Actinide(III) (Ac, Am, Cm) Aqueous Complexation Chemistry, *Chem. Sci.*, 2021, **12**(15), 5638–5654.

49 M. G. Ferrier, E. R. Batista, J. M. Berg, E. R. Birnbaum, J. N. Cross, J. W. Engle, H. S. La Pierre, S. A. Kozimor, J. S. L. Pacheco, B. W. Stein, S. C. E. Stieber and J. J. Wilson, Spectroscopic and Computational Investigation of Actinium Coordination Chemistry, *Nat. Commun.*, 2016, **7**, 1–8.

50 B. W. Stein, S. A. Kozimor, V. Mocko, D. L. Clark, D. A. Geeson and R. J. Hanrahan Jr, The Plutonium Handbook, in *The Plutonium Handbook*, American Nuclear Society, Illinois, 2019, p. 2951.

51 S. K. Cary, K. S. Boland, J. N. Cross, S. A. Kozimor and B. L. Scott, Advances in Containment Methods and Plutonium Recovery Strategies That Led to the Structural Characterization of Plutonium(IV) Tetrachloride Tris-Diphenylsulfoxide, PuCl4(OSPh2)3, *Polyhedron*, 2017, **126**, 220–226.

52 O. V. Dolomanov, L. J. Bourhis, R. J. Gildea, J. A. K. Howard and H. Puschmann, OLEX2: a complete structure solution, refinement and analysis program, *J. Appl. Crystallogr.*, 2009, **42**, 339–341.

53 G. M. Sheldrick, SHELXT - Integrated Space-Group and Crystal-Structure Determination, *Acta Crystallogr., Sect. A*, 2015, **71**(1), 3–8.

54 G. M. Sheldrick, A Short History of SHELX, *Acta Crystallogr., Sect. A: Found. Crystallogr.*, 2008, **64**(1), 112–122.

55 K. Momma and F. Izumi, VESTA 3 for Three-Dimensional Visualization of Crystal, Volumetric and Morphology Data, *J. Appl. Crystallogr.*, 2011, **44**, 1272–1276.

56 C. R. Groom, I. J. Bruno, M. P. Lightfoot and S. C. Ward, The Cambridge Structural Database, *Acta. Crystallogr., Sect. B: Struct. Sci., Cryst. Eng. Mater.*, 2016, **72**(2), 171–179.

